Chemistry & Biology, Vol. 10, 695–704, August, 2003, ©2003 Elsevier Science Ltd. All rights reserved. DOI 10.1016/S1074-5521(03)00169-8

Irreversible Inhibition of CD13/Aminopeptidase N by the Antiangiogenic Agent Curcumin

Joong Sup Shim,[1] Jin Hee Kim,[1] Hyun Young Cho,[2] Young Na Yum,[2] Seung Hee Kim,[2] Hyun-Ju Park,[3] Bum Sang Shim,[4] Seung Hoon Choi,[4] and Ho Jeong Kwon[1,*]

[1] Department of Bioscience and Biotechnology
Institute of Bioscience
Sejong University
Seoul 143-747

[2] National Institute of Toxicological Research
Korea Food and Drug Administration
Seoul 122-704

[3] College of Pharmacy
Sungkyunkwan University
Suwon 440-746

[4] College of Oriental Medicine
Kyung Hee University
Seoul 130-701
Korea

Summary

CD13/aminopeptidase N (APN) is a membrane-bound, zinc-dependent metalloproteinase that plays a key role in tumor invasion and angiogenesis. Here, we show that curcumin, a phenolic natural product, binds to APN and irreversibly inhibits its activity. The direct interaction between curcumin with APN was confirmed both in vitro and in vivo by surface plasmon resonance analysis and an APN-specific antibody competition assay, respectively. Moreover, curcumin and other known APN inhibitors strongly inhibited APN-positive tumor cell invasion and basic fibroblast growth factor-induced angiogenesis. However, curcumin did not inhibit the invasion of APN-negative tumor cells, suggesting that the antiinvasive activity of curcumin against tumor cells is attributable to the inhibition of APN. Taken together, our study revealed that curcumin is a novel irreversible inhibitor of APN that binds to curcumin resulting in inhibition of angiogenesis.

Introduction

CD13 (gp150), a myeloid cell surface glycoprotein, is identical to aminopeptidase N (APN), an ectoenzyme which can cleave bioactive proteins on the cell surface, including several cytokines [1]. It is involved in the down-regulation of signal peptides, such as enkephalines [2]. Various studies have shown that APN, as a zinc-dependent metalloproteinase, plays an important role in metastatic tumor cell invasion [3, 4]. The stable transfection of melanoma cells with full-length APN cDNA significantly increased the invasiveness of the cells. A good correlation between the invasiveness index and APN expression levels was demonstrated [3]. Functional studies on APN in tumor invasion revealed that the metalloprotease cleaves certain extracellular matrix proteins, including type IV collagen and some components of Matrigel [4, 5].

Recently, APN was identified as a receptor for a tumor-homing peptide motif, NGR (Asp-Gly-Arg), which is capable of homing selectively to the tumor vasculature [6]. The only vascular structures with detectable APN were tumor vessels and other types of vessels undergoing angiogenesis, which suggested that APN could be a novel angiogenic marker. Furthermore, several inhibitors of APN significantly inhibited hypoxia-induced retinal neovascularization, basic fibroblast growth factor (bFGF)-induced angiogenesis in the chorioallantoic membrane (CAM), and tumor growth of breast carcinoma (MDA-MB-435) xenografts in mice [6]. Since MDA-MB-435 cells are APN negative, the tumor growth inhibition by APN inhibitors appeared to be through a direct targeting of APN expressed on the tumor vasculature [6, 7]. These data indicate that APN plays a critical role in angiogenesis. Accordingly, APN is considered an important therapeutic target for tumor angiogenesis and metastasis. Based on this idea, an extensive screening was carried out to discover functional inhibitors of APN from natural products and chemical libraries [8, 9]. Here, we have identified curcumin and its derivatives as novel inhibitors of APN.

Curcumin (Figure 1) is a phenolic natural product isolated from the rhizome of *Curcuma longa* (turmeric). It consists of two vinylguaiacol groups joined by a β-diketone unit. Previous studies have shown that curcumin strongly inhibited the initiation and promotion of chemical carcinogen-induced tumor formation in mice [10, 11] and the proliferation of various cultured tumor cells [12–14]. These potent chemopreventive activities of curcumin may be attributed to the inhibition of certain signal transduction pathways critical for tumor cell growth, such as AP-1, NF-κB, and protein kinase C [15–17].

Recently, curcumin was shown to inhibit the proliferation of human umbilical vein endothelial cells (HUVECs) and to reduce the expression of matrix metalloproteinase-9 (MMP-9) [18, 19]. Moreover, curcumin inhibited corneal neovascularization without inhibiting TPA-induced secretion of vascular endothelial growth factor (VEGF) [20]. These studies demonstrate that the potent chemopreventive activity of curcumin may, in part, be derived from the direct inhibition of in vivo angiogenesis. However, the mechanism of angiogenesis inhibition by curcumin has not been fully understood yet.

Here, we show that curcumin strongly inhibits APN activity both in vitro and in vivo and directly binds to APN in vitro and in HUVECs. The inhibition of APN activity by curcumin resulted in a dose-dependent suppression of tumor invasion of APN-positive cells and of bFGF-induced angiogenic differentiation of HUVECs. These results demonstrate that APN is an important target of curcumin for its antiangiogenic activity.

*Correspondence: kwonhj@sejong.ac.kr

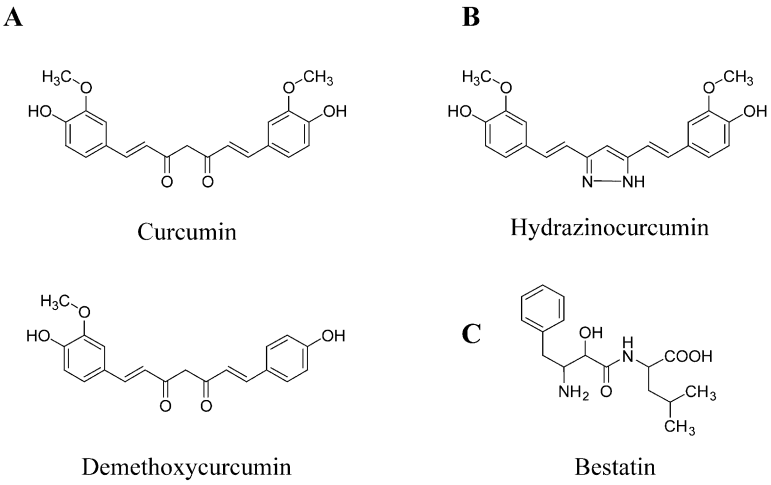

Figure 1. Structures of Compounds

(A) Curcumin and demethoxycurcumin were purified from commercial curcuminoids using thin layer chromatography.

(B) Hydrazinocurcumin is a new synthetic derivative of curcumin.

(C) Bestatin is a competitive inhibitor of APN.

Results

Curcumin Potently Inhibits APN Enzymatic Activity In Vitro and In Vivo

The screening of APN inhibitors was carried out using 3000 compounds from natural products and the chemical library in our laboratory. A final concentration of 10 μg/ml of each library was inoculated into each well of a black 96-well plate, and high-throughput screening was carried out by fluorescence measurement. In the course of the screening, curcumin was presently identified as a potent inhibitor of APN. Curcumin and its derivatives (Figure 1), including demethoxycurcumin, hydrazinocurcumin, and bestatin, a known APN inhibitor, were tested for their ability to block APN activity in vitro. Curcumin and demethoxycurcumin potently inhibited the activity of APN with IC_{50} values of 10 and 20 μM, respectively, while hydrazinocurcumin, a synthetic analog of curcumin in which the central β-diketone moiety was substituted by pyrazole, did not inhibit the enzyme activity ($IC_{50} > 100$ μM) (Figure 2A). Among the tested compounds, bestatin showed the most potent inhibitory activity against APN enzymatic activity ($IC_{50} = 2.5$ μM). The inhibition of APN by curcumin is noncompetitive ($Ki = 11.2$ μM; Figure 2B). In vivo enzyme assays were carried out by monitoring the enzymatic degradation of a fluorescent substrate using cultured cells as a source of enzyme. The in vivo specificity of the substrates, including ala-pNA and ala-7-amido-4-methylcoumarin, toward aminopeptidase N was previously demonstrated [4, 21]. Curcumin inhibited the enzymatic activity of APN both in HUVECs and in APN-positive HT1080 cells with IC_{50} values of 10 and 7 μM, respectively (Figures 2C and 2D). In the latter two assays, curcumin was more potent than bestatin, which had an IC_{50} value of 20 and 13 μM. These data demonstrate that curcumin is a noncompetitive inhibitor of APN.

Inhibition of APN Activity by Curcumin Is Irreversible

We next examined the kinetics of curcumin inhibition of APN activity. For the assay, purified APN was incubated with either curcumin or bestatin, and then the reaction mixture was filtered using a Microcon-YM30 filter, which can retain proteins higher than 30 kDa molecular weight. The retained protein in the upper part of the Microcon-YM30 filter was resuspended in PBS and examined for APN activity. The APN activity of drug-untreated control was normalized to 100% of the enzyme activity. The activity of bestatin-treated APN increased during subsequent filtration and reached about 100% of the control enzyme activity after three filtrations (Figure 3A). However, the enzymatic activity of curcumin-treated APN was not restored even after three filtrations. These data suggest that the inhibition of APN by curcumin is irreversible and that the mode of inhibition of APN by curcumin is different from that of bestatin, which is a reversible, competitive inhibitor. To further confirm the irreversibility of enzyme inhibition by curcumin, a kinetic graph (*EV* plot) of the initial velocity versus enzyme concentrations was plotted. This plot has been previously used to confirm the irreversibility of the inhibition of mammalian histone deacetylase (HDAC) by trapoxin, an antitumor cyclic tetrapeptide [22]. A similar result was obtained from the *EV* plots for curcumin and APN. As shown in Figure 3B, the enzyme activity of the control group increased in proportion to the amount of enzyme added. Treatment with 10 μM bestatin inhibited the enzyme activity at a constant ratio depending on the enzyme concentration. In contrast, 10 μM of curcumin inhibited the enzyme activity by a fixed extent irrespective of the enzyme concentrations, leading to a parallel shift of the *EV* plot line from the control line toward the right. These data suggest that a fixed amount of APN, corresponding to the amount of curcumin, was irreversibly inhibited.

Analysis of the Interaction between Curcumin and APN In Vitro and In Vivo

In vitro interaction of curcumin with APN was investigated using surface plasmon resonance analysis. A strong binding curve was observed when curcumin was applied to immobilized APN on the CM5 sensor chip (Figure 4A). As much as 100 μM hydrazinocurcumin, an inactive curcumin derivative, however, did not bind to APN. Using BIAcore evaluation software, the kinetic pa-

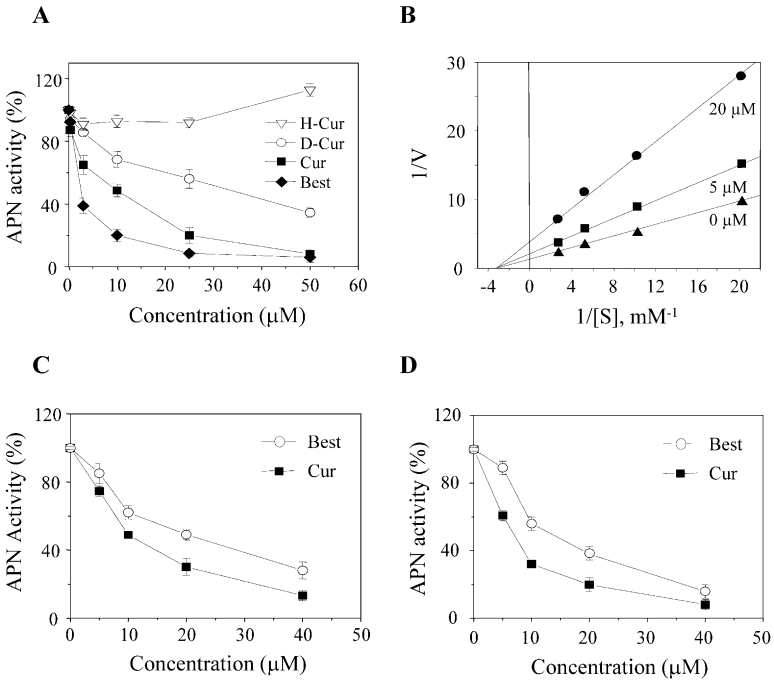

Figure 2. The Effect of Curcumin Derivatives on APN Activity

(A) In vitro APN assay using purified aminopeptidase N.

(B) Kinetic analysis of enzyme inhibition by curcumin using Lineweaver-Burk plot of APN. Dixon plot was used to determine the K*i* value (K*i* = 11.2 μM).

(C and D) In vivo enzyme assay of APN in HUVECs (C) and in HT1080 (D) cells, respectively. Each value represents mean ± SE from three independent experiments. Cur, curcumin; D-Cur, demethoxycurcumin; H-Cur, hydrazinocurcumin; Best, bestatin.

rameters of k_a, k_d, and K_D were measured. There was a very low dissociation rate (k_d) of 2.92×10^{-5} s^{-1}, whereas the association rate (k_a) was 2.98 M^{-1} s^{-1}. The apparent dissociation constant (K_D) of curcumin binding to APN was calculated as 9.8×10^{-6} M. In addition, the steady-state affinity data for curcumin were obtained from the software. Steady-state binding levels (R_{eq}) of each curcumin concentration were plotted, and the saturation curve was obtained from the plot (Figure 4B). Saturation of binding was observed from >50 μM of curcumin to APN immobilized on a CM5 sensor chip. Next, we investigated the interaction of curcumin with APN in HUVECs. To investigate the binding capacity of curcumin to APN in vivo, HUVECs treated with either curcumin or hydrazinocurcumin were harvested with EDTA and subsequently labeled with WM15, an antibody specific for human APN [23]. Antibody-labeled cells were then incubated with FITC-conjugated anti-mouse IgG and subjected to fluorescent activated cell sorting (FACS) analysis. Control, untreated cells exhibited a high level of fluorescence, shown as a dramatic shift in curves (Figure 4Ca, black arrow). However, 10 μM of curcumin significantly reduced the fluorescence level of HUVECs labeled with the antibody (Figure 4Cb). The competition of curcumin with the antibody for the binding to APN is dose dependent (Figures 4Ca, 4Cb, and 4Cc). We then investigated the effect of hydrazinocurcumin, an inactive curcumin derivative, on the competition of antibody binding to APN. Though hydrazinocurcumin is very similar to curcumin in structure and hydrophobicity, it did not change the level of fluorescence even at 50 μM treatment (Figure 4Cd). These data imply that the interaction between curcumin and APN is specific. The specificity of antibody (WM15) to APN was verified using two different cell lines, HT1080 and MDA-MB-231 cells. HT1080 cells showed a high binding affinity with the antibody (Figure 4Da), while MDA-MB-231 cells that are APN negative did not change their fluorescence level (Figure 4Db). These data demonstrate that curcumin directly binds to APN both in vitro and in vivo with high affinity and inhibits its enzymatic activity.

Curcumin Inhibits bFGF-Induced Angiogenesis

Specific inhibition of APN activity has previously been shown to suppress angiogenesis both in vitro and in vivo [6, 7]. Therefore, we examined the effects of curcumin and bestatin on angiogenesis. First, we investigated the time- and dose-response of curcumin on HUVEC growth. Curcumin inhibited the proliferation of HUVECs in a time- and dose-dependent manner (Figure 5A). Cytotoxicity was not observed at 15 μM treatment for 72 hr. Thus, all angiogenesis assays were conducted at the concentration range of 1 to 15 μM within 72 hr. We then examined the effects of APN inhibitors on angiogenesis using in vitro invasion and tube formation assays. Curcumin and bestatin inhibited bFGF-induced invasion (Figure 5B) and capillary tube formation of HUVECs (Figures 5Cb, 5Cc [white arrow], and 5Cd) in a dose-dependent manner. Cytotoxicity was not observed in tube formation assay as confirmed by trypan blue staining (data not shown). Furthermore, in vivo endogenous neovascularization of the chick embryonic chorioallantoic membrane was significantly blocked by curcumin without showing rupture of preexisting vessels (Figure 5D). Negligible toxicity toward eggs was observed after curcumin treatment, indicating that the compound is a promising, nontoxic antiangiogenic agent.

Analysis of APN Expression and Tumor Cell Invasion

We then examined the expression of APN in HUVECs to determine whether its expression is regulated with angiogenic differentiation induced by bFGF. RT-PCR analysis showed that bFGF significantly increased the

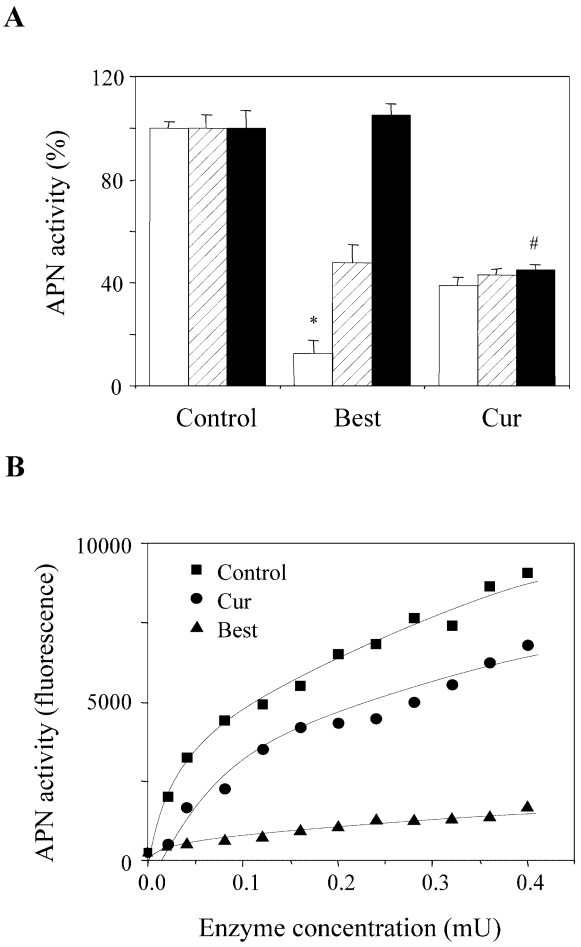

Figure 3. Reversibility and Kinetic Analysis of APN Inhibition by Curcumin

(A) Reversibility of enzyme inhibition. Purified porcine APN was incubated with 0.5% methanol (Control), 10 μM bestatin (Best), and 10 μM curcumin (Cur) for 2 hr. The enzyme reaction solutions were filtered using Microcon-YM30, and the activity of the residual enzyme resuspended in PBS was determined. The white bars represent the enzymatic activity of APN before the filtration. The hatched and black bars represent the enzymatic activity of APN after the filtration one and three times, respectively. The APN activity of drug-untreated control was normalized to 100%, and drug-treated enzyme activity was expressed as a percentage of inhibition versus control. The data represent mean ± SE from three independent experiments. *, $p < 0.0001$ versus control APN activity (before filtration); #, $p < 0.0004$ versus control APN activity (after filtration three times).

(B) Kinetics analysis of enzyme inhibition. The enzymatic activity of APN was determined as described in Experimental Procedures. The kinetics of enzyme inhibition by bestatin (Best) or curcumin (Cur) is presented as an *EV* plot of initial velocity versus enzyme concentrations.

expression level of APN in HUVECs (Figures 6A and 6B), in agreement with a previous report by Bhagwat et al. [7]. Various tumor cell lines were also investigated to determine the expression level of APN. As shown in Figure 6C, C8161, a human melanoma, HT1080, a human fibrosarcoma, and B16/BL6, a murine melanoma, showed high levels of APN expression, whereas HT29 and HCT116, colon carcinomas, and MCF-7 and MDA-MB-231, breast cancer cells, showed relatively low amounts or absence of APN expression. Several investigations suggest that APN plays a pivotal role in tumor metastasis, which is supported by reports that several APN inhibitors, including bestatin, actinonin, amastatin, and homophthalimide, blocked metastatic tumor cell invasion [5, 24, 25]. The relationship between APN expression and cell invasive activity was investigated. The relative invasiveness of each tumor cell was determined by comparison with that of HT1080 cells used as a normalization control (100%). The results revealed that APN-expressing C8161 and B16/BL6 cells were highly invasive, while HT29 and HCT116 cells that were APN negative showed relatively low invasive activities (Figure 6D). In contrast, breast cancer cells were highly invasive, even though they showed low amounts of APN expression or were APN negative. Since the degradation of the extracellular matrix involves several proteases, including matrix metalloproteinases, serine proteases, and aminopeptidases, the invasiveness of breast cancer cells seems to be APN independent [26].

Curcumin Inhibits Tumor Invasion of APN-Positive Cells but Does Not Affect an APN-Negative Cell Line

We finally examined the functional significance of APN inhibition by curcumin using two cell lines showing different expression levels of APN. APN-positive (C8161) and -negative (MDA-MB-231) tumor cells were used to investigate the effect of curcumin on the invasiveness of the cells. Both cell lines were highly invasive, as shown in Figure 6D. Interestingly, C8161 cell invasion was significantly inhibited by curcumin, whereas that of MDA-MB-231 cells was not (Figure 7A). The inhibition of the invasion of C8161 cells occurred at a concentration of 5 μM (Figure 7), which was found to inhibit the enzymatic activity of APN (Figure 2). In addition, tumor invasion of all three APN-positive cells was significantly inhibited by curcumin without showing any cytotoxicity at the same concentration (Figure 7B). These results suggest that curcumin inhibits the invasion of APN-positive cells, at least in part, through the inhibition of the enzymatic activity of APN.

Discussion

Curcumin is a potent chemopreventive agent that has been entered into phase I clinical trials for cancer chemoprevention by the National Cancer Institute, NIH, Bethesda, MD [27]. Many other groups also reported phase I clinical trials of curcumin and showed promising results, i.e., curcumin is pharmacologically safe and has enormous potential in the prevention and therapy of cancer [28–30]. Because its chemopreventive activities have been observed at various tumor types [10, 11], it has been postulated that the potent chemopreventive activity of curcumin may be, in part, the result of a direct inhibition of angiogenesis [20], which would be widely effective on the growth of tumors in vivo [31]. However, the molecular basis for the precise mechanism of angiogenesis inhibition by curcumin has not yet been elucidated.

In the present study, we found that curcumin binds

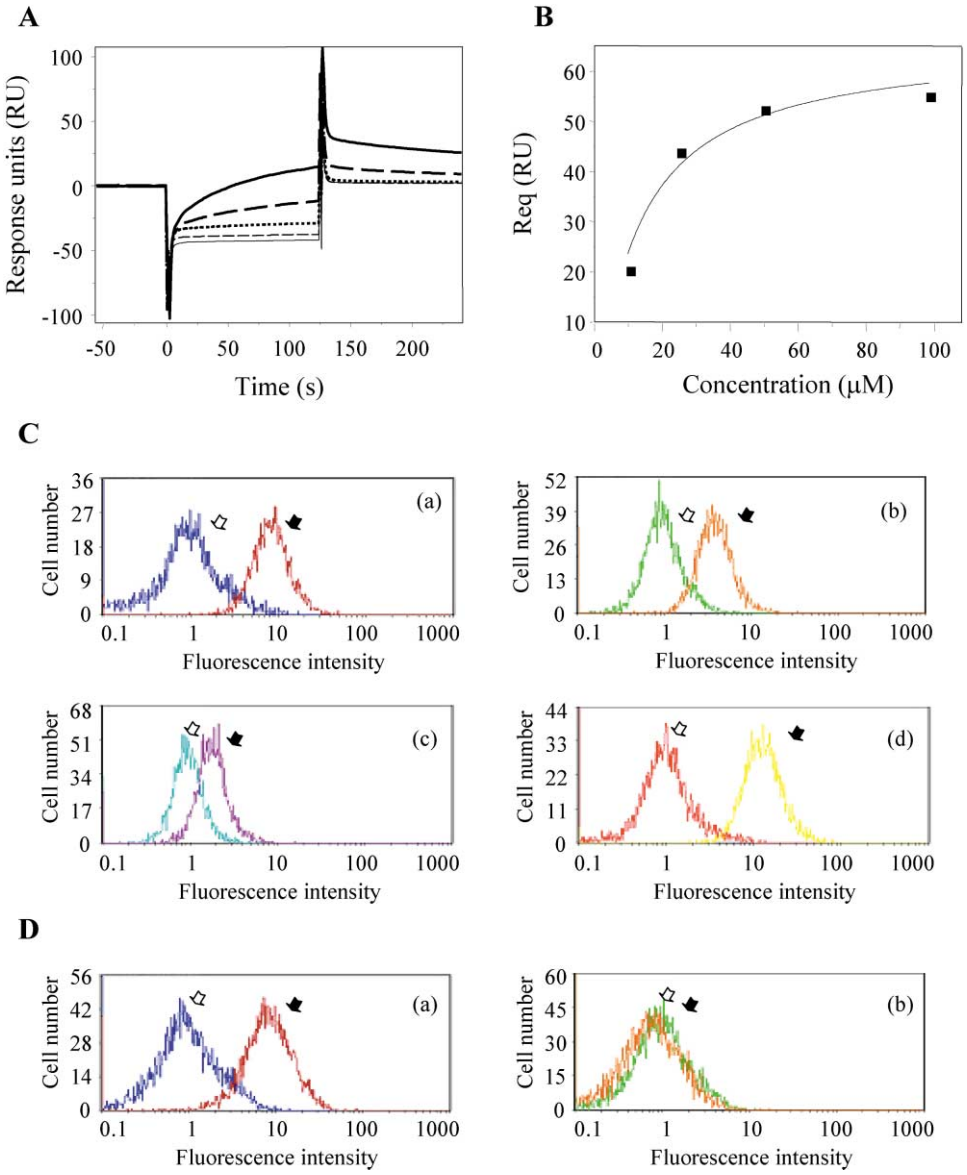

Figure 4. Analysis of the Interaction Between Curcumin and APN In Vitro and In Vivo

(A) The binding sensorgram of the curcumin and hydrazinocurcumin on APN from BIAcore analysis. Sensorgrams were obtained for 4 μM (bold dotted line), 16 μM (bold broken line), and 50 μM (bold line) of curcumin, 100 μM of hydrazinocurcumin (thin broken line), and 5% DMSO in flow buffer (thin line) against APN immobilized on the sensor chip.

(B) The plot of steady-state binding level (R_{eq}) against the concentration of curcumin. Each value was obtained from the equation as described in Experimental Procedures.

(C) FACS analysis of the competitive binding of curcumin with APN-specific antibody (WM15) to HUVECs. The curves indicated by white arrows represent HUVECs incubated with FITC-conjugated anti-mouse IgG only. Black arrows indicate the curves for HUVECs labeled with WM15 followed by FITC-conjugated anti-mouse IgG. Curves were obtained from antibody-labeled HUVECs incubated with 0 μM (a), 10 μM (b), and 50 μM (c) of curcumin and 50 μM of hydrazinocurcumin (d).

(D) The binding of WM15 to APN in either HT1080 (APN-positive) or MDA-MB-231 (APN-negative) cells. Note the increased fluorescence in HT1080 (a) but not in MDA-MB-231 cells (b).

to APN and irreversibly inhibits its activity. The direct interaction between curcumin and APN was confirmed in vitro and in vivo by surface plasmon resonance analysis and an antibody competition assay. However, the mode of binding of curcumin to APN has not yet been determined. Several studies suggest that α, β-unsaturated ketones of curcumin are crucial for the binding to its target proteins. Various thiol compounds, including cysteine, dithiothreitol, and β-mercaptoethanol, are known to cause the reduction of curcumin, and reduced curcumin could not inhibit the activation of protein kinase C [17]. Protein kinase C contains cysteine residues located in its regulatory domain, which may form an adduct with the α, β-unsaturated ketones of curcumin [17]. In addition, human glutathione S-transferase P1-1 (GSTP1-1) is irreversibly inhibited by cur-

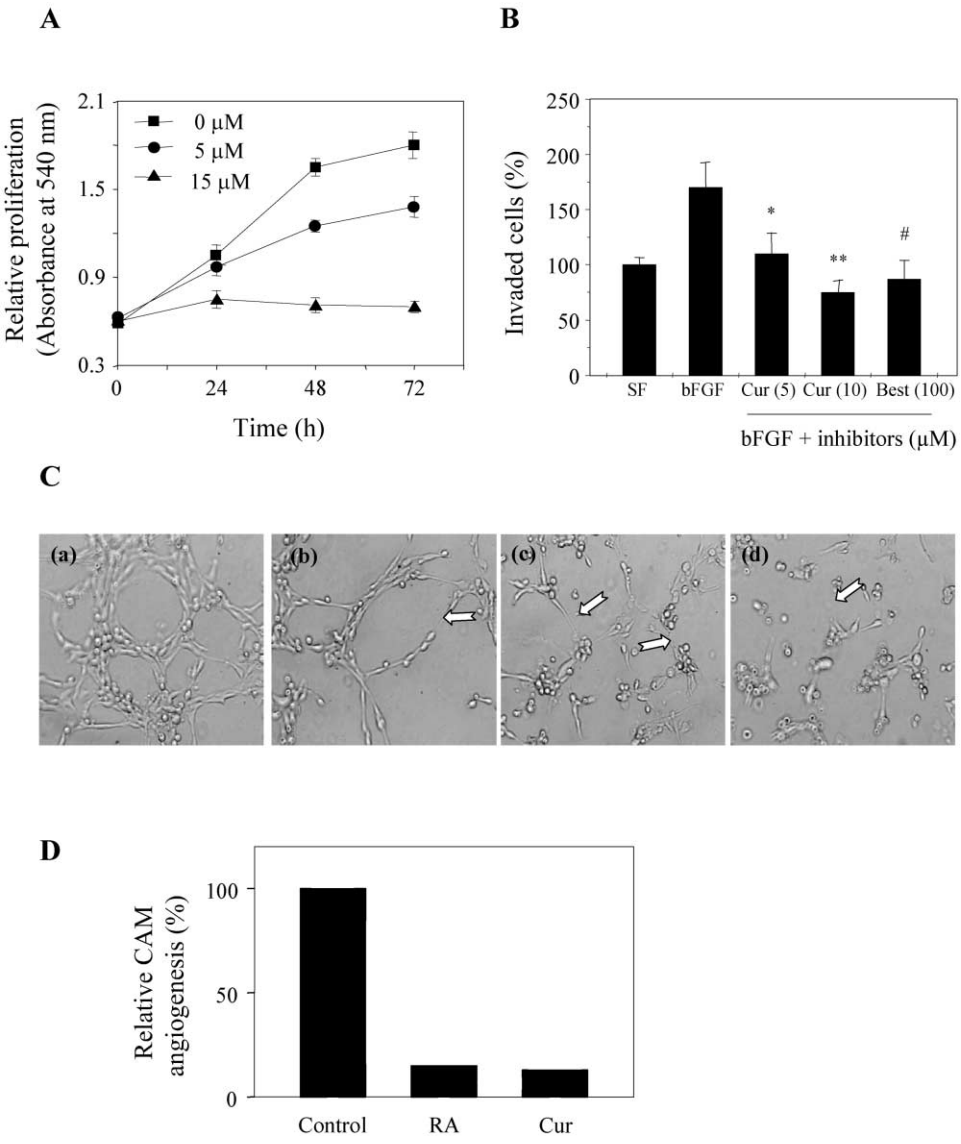

Figure 5. Inhibition of Angiogenesis Activities by Curcumin and Bestatin

(A) Time and dose responses of curcumin on HUVECs. HUVECs were treated with curcumin, and cell growth was determined at various time points. The absorbance of MTT-formazan (540 nm, *y* axis) represents cell growth. Each value represents mean ± SE from three independent experiments.

(B) The effects of curcumin and bestatin on the bFGF-induced invasion of HUVECs. Serum-starved HUVECs in serum-free medium (SF) or treated with bFGF in the presence or absence of inhibitors were used for invasion assay. The invasiveness of cells in SF was used as a normalization control (100%). Each value represents the mean ± SE from three independent experiments. *, $p < 0.03$; **, $p < 0.007$; and #, $p < 0.02$ versus bFGF control.

(C) The effects of curcumin and bestatin on capillary tube formation of HUVECs. HUVECs with 30 ng/ml of bFGF (a), bFGF and 5 μM curcumin (b), bFGF and 10 μM curcumin (c), and bFGF and 100 μM bestatin (d). White arrows indicate the inhibition of tube networks by the agents.

(D) Inhibition of angiogenesis by curcumin in the CAM assay. Retinoic acid (RA, 1 μg/egg) and curcumin (Cur, 10 μg/egg) were applied to the CAM assay, and the inhibition ratio was calculated based on the percentage of angiogenic eggs to total numbers of eggs tested.

cumin through the Michael addition of the Cys^{47} residue in GSTP1-1 with α, β-unsaturated ketones of the compound [32]. Interestingly, the M_1 family of zinc metallopeptidases, including pig APN, human APN, human aminopeptidase A (APA), rat aminopeptidase B (APB), and mouse puromycin-sensitive aminopeptidase (PSA), have four highly conserved domains in the active site of the enzymes [33]. These conserved domains contain two nucleophilic amino acid residues, Cys^{218} and Lys^{225}. In our study, the reduction of curcumin by thiol compounds, particularly by cysteine, completely blocked the inhibitory activity of curcumin against APN (data not shown). Thus, we postulate that α, β-unsaturated ketones of curcumin may be covalently linked to nucleophilic amino acid residues in the active site of APN.

To investigate a possible binding mode of curcumin and its derivatives to APN, flexible dockings were conducted using the FlexX program implanted in Sybyl 6.8

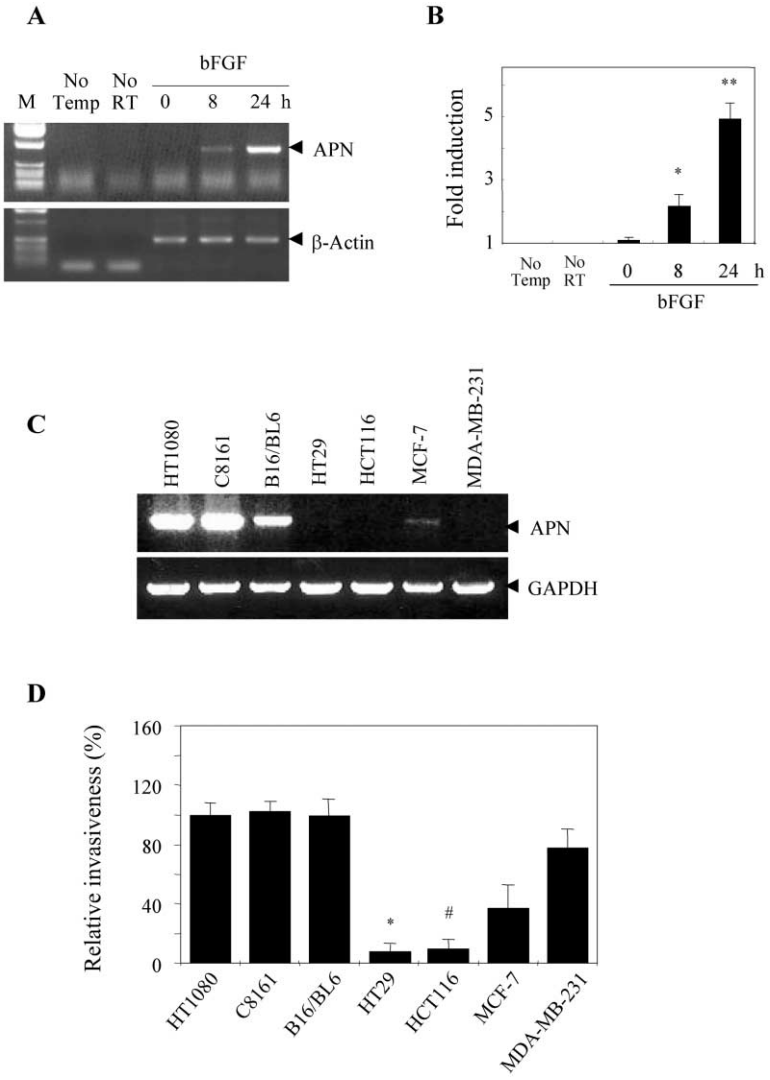

Figure 6. Analysis of APN Expression and Tumor Invasion

(A) RT-PCR analysis of APN expression in HUVECs. HUVECs were stimulated by bFGF (30 ng/ml), and RNA was isolated at the indicated time points. The isolated RNA was converted to cDNA in the presence or absence (No RT) of reverse transcriptase. Standard RT-PCR was performed using the primer pair specific for APN with or without (No Temp) cDNA template. The level of β-actin mRNA was used as an internal control. M denotes size marker.

(B) Quantitative data for RT-PCR results. The expression level of APN mRNA was determined by densitometry. Each value represents mean ± SE from three independent experiments. *, $p < 0.04$; **, $p < 0.0004$ versus bFGF (0 hr).

(C) APN expression in cultured tumor cell lines using RT-PCR with primers common to murine and human APN. The level of glyceraldehyde-3-phosphate dehydrogenase (GAPDH) mRNA was used as an internal control.

(D) Relative invasiveness of various tumor cell lines. The invasiveness of each cell line was determined by the ratio of the number of invaded cells to total inoculated cells. Relative invasiveness of each cell line was calculated by the comparison with the invasiveness of HT1080 cells that were used as a normalization control (100%). Tumor invasion assay was performed as described in Experimental Procedures. Each value represents mean ± SE from three independent experiments. *, $p < 0.0001$; #, $p < 0.0002$ versus HT1080 control.

(Tripos Inc.) (J. Lee, J.S.S, H.-J.P., and H.J.K, unpublished results). The active site of bovine lens leucine aminopeptidase (blLAP, EC.3.4.11.1), the only aminopeptidase for which an X-ray structure is available [34], was introduced into the docking study. In enzyme assays, the activity of blLAP was inhibited by curcumin similar to the level observed with APN (data not shown). In docking studies, curcumin snugly fits into the catalytic pocket of blLAP. The active site of blLAP contains two lysine residues (Lys^{250} and Lys^{262}) that may form an adduct with curcumin through Michael addition or Schiff-base formation. In contrast, hydrazinocurcumin, a conformationally rigid derivative, fails to be accommodated into the catalytic pocket of blLAP, based on data showing that hydrazinocurcumin fails to inhibit APN activity.

Basement membrane degradation by proteases is an essential step for both tumor cell invasion and angiogenesis. APN, as a matrix degrading zinc metallopeptidase, is crucially involved in tumor cell invasion and angiogenesis [3–7]. Thus, the inhibition of APN activity was regarded as sufficient to suppress angiogenesis [6, 7]. Our data showed that curcumin strongly inhibited both the invasion of APN-positive tumor cells and growth factor-induced angiogenesis of endothelial cells at the same concentration at which the inhibition of APN activity occurred. However, the invasion of APN-negative breast cancer cells was not inhibited by curcumin. These data suggest that APN is a direct target of curcumin for its antiinvasive activity. Considering that endothelial cell invasion is an essential step for angiogenesis, the antiangiogenic activity of curcumin is also through, in part, the inhibition of APN activity. However, we cannot exclude the possibility that curcumin still affects other known cellular targets, such as PKC and Ca^{2+}-ATPase [35], and certain signal transduction pathways that are possibly involved during the complex process of angiogenesis [15–17, 36, 37]. Thus, we speculate that in vivo inhibition of angiogenesis by curcumin may be a consequence of multiple effects against several targets required for angiogenesis, including APN. Our results demonstrate aminopeptidase N as a new direct binding target of curcumin for its antiangiogenic activity. These data will help to decipher the mode of actions of this clinically promising agent.

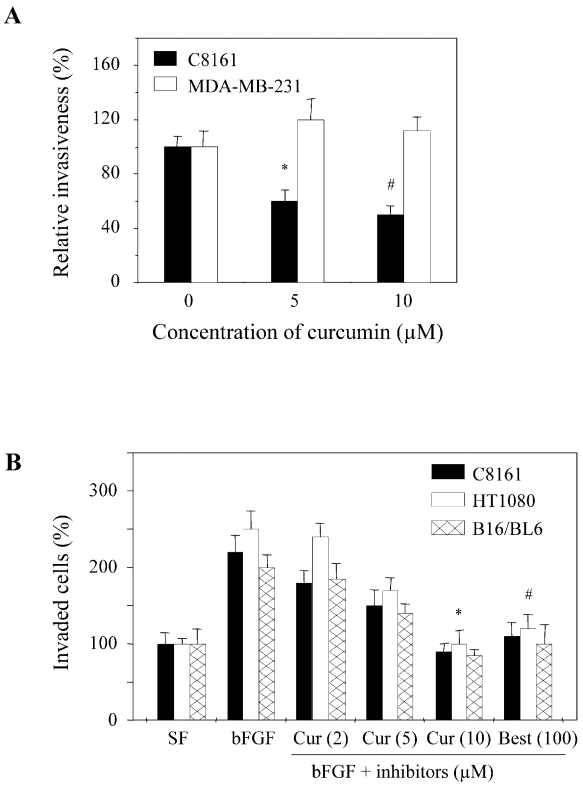

Figure 7. Curcumin Inhibits Tumor Invasion of APN-Positive Cells but Does Not Affect an APN-Negative Cell Line

(A) Effect of curcumin on C8161 and MDA-MB-231 cell invasion. The number of cells that invaded was determined using a microscope, and the data are presented as the average number of invaded cells. The invasiveness of each cell line without curcumin treatment was used as a normalization control (100%). *, $p < 0.003$ versus C8161 control; #, $p < 0.0002$ versus MDA-MB-231 cells treated with 10 μM curcumin.

(B) Effects of curcumin and bestatin on bFGF-induced tumor invasion of three APN-positive cell lines. The invasiveness of each cell line in serum-free media was used as a normalization control (100%). Each value represents mean ± SE from three independent experiments. *, $p < 0.0006$; #, $p < 0.001$ versus bFGF-stimulated HT1080 control.

Significance

Angiogenesis is the formation of new blood vessels from preexisting vasculature. This process is essential for tissue growth, wound repair, tumor growth, and metastasis. APN is a membrane-bound, zinc-dependent metalloproteinase that is believed to play a key role in tumor invasion and angiogenesis. Accordingly, APN is considered an important therapeutic target for tumor angiogenesis and metastasis. The present study demonstrates for the first time that curcumin, a potent chemopreventive agent in phase I clinical trials, binds to APN and irreversibly inhibits its activity. The direct interaction between curcumin and APN was confirmed by in vitro and in vivo assays. Furthermore, curcumin and other known APN inhibitors strongly inhibited APN-positive tumor cell invasion and basic fibroblast growth factor-induced angiogenesis. However, curcumin did not significantly inhibit the invasion of APN-negative tumor cells, suggesting that the anti-invasive activity of curcumin against tumor cells is attributable to the inhibition of APN. Thus, our study reveals that curcumin is a novel irreversible inhibitor of APN and provides a new mode of action of curcumin for its antiangiogenic activity. Furthermore, this study strongly supports the idea that the targeted inhibition of APN activity is a novel approach to prevent tumor angiogenesis and metastasis. It may also be possible to develop potent derivatives of curcumin, since APN has been defined as the functional target of the compound for antiangiogenesis.

Experimental Procedures

Materials

Aminopeptidase N (APN), curcumin, bestatin, and ala-7-amido-4-methylcoumarin were purchased from Sigma (St. Louis, MO). WM15 (mouse monoclonal anti-human APN) was obtained from BD PharMingen (San Diego, CA). Sensor chip CM5 and the Amine Coupling Kit were obtained from BIAcore AB (Uppsala, Sweden). Basic fibroblast growth factor (bFGF) was obtained from Upstate Biotechnology (Lake Placid, NY), cell culture media from Life Technology (Grand Island, NY), Matrigel from Collaborative Biomedical Products (Bedford, MA), Transwell plates from Corning Costar (Cambridge, MA), Complete Mini protease inhibitor cocktail from Roche (Mannheim, Germany), and Microcon-YM30 from Millipore (Bedford, MA). Hydrazinocurcumin, an inactive analog of curcumin, was prepared by a chemical modification of curcumin as reported previously [38].

Cell Culture and Growth Assay

Early passages (4–8 passages) of human umbilical vein endothelial cells (HUVECs) were kindly provided by Dr. Y.G. Kwon at Kangwon National University. HUVECs were grown in Medium-199 supplemented with 20% fetal bovine serum (FBS), 5 units/μl of heparin, and 1% bFGF. C8161, HT1080, MCF-7, and MDA-MB-231 cells were maintained in DMEM, and B16/BL6, HT29, and HCT116 cells were grown in RPMI1640 containing 10% FBS. The proliferation of HUVECs was measured using a 3-(4,5-dimethylthiazol-2-yl)-2,5-diphenyltetrazolium bromide (MTT) assay, and the cytotoxicity was assessed using trypan blue staining as described previously [38].

Assay of APN Activity

The activity of APN was determined according to the method described by Saiki et al. [4]. Briefly, the enzyme substrate, ala-7-amido-4-methylcoumarin (0.1 mM), was added to phosphate buffered saline (PBS) with or without inhibitors. The reaction was initiated by adding an enzyme solution (final concentration, 2×10^{-4} unit) and continued in a darkroom at 37°C. After 1 hr, the mixture was centrifuged and the supernate was collected for the measurement of fluorescence using a FL600 microplate fluorescence reader (Bio-Tek Instrument Inc, Winooski, VT) at the excitation and emission wavelengths of 360 and 460 nm, respectively. For in vivo cell-based enzyme assay, cells (2×10^5) were seeded in each well of a 24-well culture plate, and after incubation for 24 hr culture medium in each well was replaced with 500 μl of PBS. Substrates (0.1 mM) were added directly into each well with or without inhibitors, and the plate was incubated in a darkroom at 37°C for 1 hr. The supernate from each well was collected, and enzyme activity was determined as described above.

Reversibility of APN Inhibition

Purified APN was incubated with or without test compounds at 4°C for 2 hr. Each reaction solution was then applied to a Microcon-YM30 filter and centrifuged for 10 min at 10,000 ×g. The residual enzyme solution retained in the upper part of the Microcon-YM30 filter was resuspended in PBS and examined for APN activity. Each resuspended enzyme solution was further applied to a Microcon-YM30 filter, and the residual enzyme activity was measured. The filtration steps were performed three times. At each step, the APN activity of drug-untreated control was normalized to 100%, and

drug-treated enzyme activity was expressed as a percentage of inhibition versus each control.

SPR Analysis

Purified porcine APN was covalently linked to a CM5 sensor chip with the Amine Coupling Kit. The surface matrix was activated by a 7 min injection of an aqueous solution of 0.2 M N-ethyl-N′-(3-diethylaminopropyl)-carbodiimide (EDC) and 50 mM N-hydroxysuccinimide (NHS). Then, APN (100 μg/ml) diluted in sodium acetate buffer (pH 4.5) was injected into the sensor cells. All coupling reactions were performed at a flow rate of 5 μl/min. Remaining N-hydroxysuccinimide-ester groups were inactivated by injection of 1.0 M ethanolamine-HCl (pH 8.5) for 10 min. For the binding analysis, samples in the running buffer (10 mM HEPES [pH 7.4], 150 mM NaCl, and 3 mM EDTA) containing 5% DMSO were injected at a flow rate of 30 μl/min. Association and dissociation curves were obtained on a BIAcore 3000. The surface of the sensor chip was regenerated by injection of 10 μl of the regeneration buffer (10 mM NaCl and 0.1 mM NaOH). The surface plasmon resonance (SPR) response curves were analyzed with BIAcore Evaluations software, version 3.1. The dissociation rate constant (k_d) was determined from a plot of $\ln(R_0/R)$ versus time, with R being the surface plasmon resonance signal at time t; the association rate constant (k_a) was determined from a plot of ln(abs(dR/dt)) versus time. The apparent association and dissociation constants were calculated from the kinetic constants: $K_A = k_a/k_d$, $K_D = k_d/k_a$. The steady-state binding level (R_{eq}) is related to the concentration (C) of analyte according to the equation $R_{eq} = K_A\, CR_{max}/1 + K_A\, Cn$. R_{max} is the theoretical binding capacity, which will differ from an experimentally measured value if *n* is not equal to 1. Then, R_{eq} against C was plotted to create the saturation curve for curcumin binding to APN.

FACS Analysis

HUVECs were harvested using PBS containing 2 mM EDTA and treated with curcumin or hydrazinocurcumin. After washing with PBS, the cells were fixed with 4% paraformaldehyde for 30 min at 4°C. After washing with fluorescence activated cell sorting (FACS) buffer containing 1% BSA and 0.1% NaN_3 in PBS, the cells were labeled with the antibody WM15 and subsequently with FITC-conjugated anti-mouse IgG. As a negative control, a group of cells was labeled with FITC-conjugated secondary antibody alone. The labeled cells were washed with FACS buffer and analyzed on a Coulter Epics XL/XL-MCL flow cytometer system (Beckman Coulter, Fullerton, CA).

In Vitro Endothelial Cell Tube Formation Assay

In vitro capillary tube formation of endothelial cells was carried out as described previously [39, 40]. Briefly, HUVECs (1×10^5 cells) inoculated on the surface of the Matrigel in a 48-well plate were treated for 6–18 hr with the indicated compounds in the presence or absence of bFGF. The tubular structures that formed were observed under a microscope and photographed at 100× magnification using a JVC digital camera (Victor, Yokohama, Japan).

Chemoinvasion Assay

The invasiveness of endothelial or tumor cells was examined in vitro using a Transwell chamber system with 8.0 μm pore-sized polycarbonate filter inserts, as described previously [39]. The total number of invaded cells on the lower side of the filter was counted using an optical microscope at 100× magnification.

CAM Assay

The chorioallantoic membrane (CAM) assay was performed as described previously [40]. Briefly, fertilized chick eggs were kept in a humidified incubator at 37°C for 3 days. About 2 ml of egg albumin was removed with a hypodermic needle, allowing the CAM and yolk sac to drop away from the shell membrane. On day 3.5, a 2.5 cm diameter window was made with a razor and tweezers, and the shell membrane was peeled away. On day 4.5, curcumin-loaded thermanox coverslips were air dried and applied to the CAM surface. Two days later, 2 ml of whipping cream mixed 1:1 with PBS was injected beneath the chorioallantoic membrane, and the CAM was observed under a microscope. Retinoic acid was used as a positive control.

RNA Preparation and Reverse Transcriptase-Polymerase Chain Reaction

Total cellular RNA was reversely transcribed by Molony murine leukemia virus reverse transcriptase (Life Technologies, Rockville, MD) using Oligo-$d(T)_{15}$ primers (Life Technologies). To determine the mRNA content of APN in each cell line, a standard PCR was performed using 5′-CCTTCAACCTGGCCAGTGC-3′ and 5′-CGTCTTCTCCAG GGCTTGCTCC-3′ as primers. The PCR products were resolved through 1% agarose gel electrophoresis and visualized by ethidium bromide staining. The mRNA level of either β-actin or glyceraldehyde-3-phosphate dehydrogenase (GAPDH) was used as an internal control.

Statistical Analysis

Results are expressed as the mean ± standard error (SE). Student's t test was used to determine statistical significance between control and test groups. A p value of <0.05 was considered statistically significant.

Acknowledgments

We are grateful to Drs. H. Kleinman, J.D. Dawson, and T.K. Kim for their critical reading of the manuscript. This study was supported by a grant from the Ministry of Health & Welfare, Republic of Korea (HMP-99-D-01-0004) and the Brain Korea 21 Project.

Received: April 24, 2003
Revised: June 2, 2003
Accepted: June 10, 2003
Published online: July 23, 2003

References

1. Look, A.T., Ashmun, R.A., Shapiro, L.H., and Peiper, S.C. (1989). Human myeloid plasma membrane glycoprotein CD13 (gp150) is identical to aminopeptidase N. J. Clin. Invest. *83*, 1299–1307.
2. Matsas, R., Stephenson, S.L., Hryszko, J., Kenny, A.J., and Turner, A.J. (1985). The metabolism of neuropeptides. Biochem. J. *231*, 445–449.
3. Fujii, H., Nakajima, M., Saiki, I., Yoneda, J., Azuma, I., and Tsuruo, T. (1995). Human melanoma invasion and metastasis enhancement by high expression of aminopeptidase N/CD13. Clin. Exp. Metastasis *13*, 337–344.
4. Saiki, I., Fujii, H., Yoneda, J., Abe, F., Nakajima, M., Tsuruo, T., and Azuma, I. (1993). Role of aminopeptidase N (CD13) in tumor-cell invasion and extracellular matrix degradation. Int. J. Cancer *54*, 137–143.
5. Menrad, A., Speicher, D., Wacker, J., and Herlyn, M. (1993). Biochemical and functional characterization of aminopeptidase N expressed by human melanoma cells. Cancer Res. *53*, 1450–1455.
6. Pasqualini, R., Koivunen, E., Kain, R., Lahdenranta, J., Sakamoto, M., Stryhn, A., Ashmun, R.A., Shapiro, L.H., Arap, W., and Ruoslahti, E. (2000). Aminopeptidase N is a receptor for tumor-homing peptides and a target for inhibiting angiogenesis. Cancer Res. *60*, 722–727.
7. Bhagwat, S.V., Lahdenranta, J., Giordano, R., Arap, W., Pasqualini, R., and Shapiro, L.H. (2001). CD13/APN is activated by angiogenic signals and is essential for capillary tube formation. Blood *97*, 652–659.
8. Kwon, H.J., Shim, J.S., Kim, J.H., Cho, H.Y., Yum, Y.N., Kim, S.H., and Yu, J. (2002). Betulinic acid inhibits growth factor-induced *in vitro* angiogenesis via the modulation of mitochondrial function in endothelial cells. Jpn. J. Cancer Res. *93*, 417–425.
9. Hashida, H., Takabayashi, A., Kanai, M., Adachi, M., Kondo, K., Kohno, N., Yamaoka, Y., and Miyake, M. (2002). Aminopeptidase N is involved in cell motility and angiogenesis: its clinical significance in human colon cancer. Gastroenterology *122*, 376–386.
10. Huang, M.T., Lou, Y.R., Ma, W., Newmark, H.L., Reuhl, K.R.,

and Conney, A.H. (1994). Inhibitory effects of dietary curcumin on forestomach, duodenal, and colon carcinogenesis in mice. Cancer Res. *54*, 5841–5847.

11. Conney, A.H., Lysz, T., Ferraro, T., Abidi, T.F., Manchand, P.S., Laskin, J.D., and Huang, M.T. (1991). Inhibitory effect of curcumin and some related dietary components on tumor promotion and arachidonic acid metabolism in mouse skin. Adv. Enzyme Regul. *31*, 385–396.
12. Khar, A., Ali, A.M., Pardhasaradhi, B.V.V., Begum, Z., and Anjum, R. (1999). Antitumor activity of curcumin is mediated through the induction of apoptosis in AK-5 tumor cells. FEBS Lett. *445*, 165–168.
13. Mehta, K., Pantazis, P., McQueen, T., and Aggarwal, B.B. (1997). Antiproliferative effect of curcumin (diferuloylmethane) against human breast tumor cell lines. Anticancer Drugs *8*, 470–481.
14. Shim, J.S., Lee, H.J., Park, S.S., Cha, B.G., and Chang, H.R. (2001). Curcumin-induced apoptosis of A-431 cells involves caspase-3 activation. J. Biochem. Mol. Biol. *34*, 189–193.
15. Huang, T.S., Lee, S.C., and Lin, J.K. (1991). Suppression of c-jun/AP-1 activation by an inhibitor of tumor promotion in mouse fibroblast cells. Proc. Natl. Acad. Sci. USA *88*, 5292–5296.
16. Singh, S., and Aggarwal, B.B. (1995). Activation of transcription factor NF-kappa B is suppressed by curcumin. J. Biol. Chem. *270*, 24995–25000.
17. Liu, J.Y., Lin, S.J., and Lin, J.K. (1993). Inhibitory effects of curcumin on protein kinase C activity induced by 12-O-tetradecanoylphorbol-13-acetate in NIH3T3 cells. Carcinogenesis *14*, 857–861.
18. Thaloor, D., Singh, A.K., Sidhu, G.S., Prasad, P.V., Kleinman, H.K., and Maheshwari, R.K. (1998). Inhibition of angiogenic differentiation of human umbilical vein endothelial cells by curcumin. Cell Growth Differ. *9*, 305–312.
19. Mohan, R., Sivak, J., Ashton, P., Russo, L.A., Pham, B.Q., Kasahara, N., Raizman, M.B., and Fini, M.E. (2000). Curcuminoids inhibit the angiogenic response stimulated by fibroblast growth factor-2, including expression of matrix metalloproteinase gelatinase B. J. Biol. Chem. *275*, 10405–10412.
20. Arbiser, J.L., Klauber, N., Rohan, R., van Leeuwen, R., Huang, M.T., Fisher, C., Flynn, E., and Byers, H.R. (1998). Curcumin is an *in vivo* inhibitor of angiogenesis. Mol. Med. *4*, 376–383.
21. Ashmun, R.A., and Look, A.T. (1990). Metalloprotease activity of CD13/aminopeptidase N on the surface of human myeloid cells. Blood *75*, 462–469.
22. Kijima, M., Yoshida, M., Sugita, K., Horinouchi, S., and Beppu, T. (1993). Trapoxin, an antitumor cyclic tetrapeptide, is an irreversible inhibitor of mammalian histone deacetylase. J. Biol. Chem. *268*, 22429–22435.
23. Bradstock, K.F., Favaloro, E.J., Kabral, A., Kerr, A., Hughes, W.G., and Musgrove, E. (1985). Myeloid progenitor surface antigen identified by monoclonal antibody. Br. J. Haematol. *61*, 11–20.
24. Yoneda, J., Saiki, I., Fujii, H., Abe, F., Kojima, Y., and Azuma, I. (1992). Inhibition of tumor invasion and extracellular matrix degradation by ubenimex (bestatin). Clin. Exp. Metastasis *10*, 49–59.
25. Kagechika, H., Komoda, M., Fujimoto, Y., Koiso, Y., Takayama, H., Kadoya, S., Miyata, K., Kato, F., Kato, M., and Hashimoto, Y. (1999). Potent homophthalimide-type inhibitors of B16F10/L5 mouse melanoma cell invasion. Biol. Pharm. Bull. *22*, 1010–1012.
26. Benbow, U., Schoenermark, M.P., Orndorff, K.A., Givan, A.L., and Brinckerhoff, C.E. (1999). Human breast cancer cells activate procollagenase-1 and invade type I collagen: invasion is inhibited by all-trans retinoic acid. Clin. Exp. Metastasis *17*, 231–238.
27. Kelloff, G.J., Crowell, J.A., Hawk, E.T., Steele, V.E., Lubet, R.A., Boone, C.W., Covey, J.M., Doody, L.A., Omenn, G.S., Greenwald, P., et al. (1996). Strategy and planning for chemopreventive drug development: clinical development plans II. J. Cell. Biochem. *26* (*suppl.*), 54–71.
28. Sharma, R.A., McLelland, H.R., Hill, K.A., Ireson, C.R., Euden, S.A., Manson, M.M., Pirmohamed, M., Marnett, L.J., Gescher, A.J., and Steward, W.P. (2001). Pharmacodynamic and pharmacokinetic study of oral Curcuma extract in patients with colorectal cancer. Clin. Cancer Res. *7*, 1894–1900.
29. Cheng, A.L., Hsu, C.H., Lin, J.K., Hsu, M.M., Ho, Y.F., Shen, T.S., Ko, J.Y., Lin, J.T., Lin, B.R., Ming-Shiang, W., et al. (2001). Phase I clinical trial of curcumin, a chemopreventive agent, in patients with high-risk or pre-malignant lesions. Anticancer Res. *21*, 2895–2900.
30. Aggarwal, B.B., Kumar, A., and Bharti, A.C. (2003). Anticancer potential of curcumin: preclinical and clinical studies. Anticancer Res. *23*, 363–398.
31. Folkman, J. (1989). What is the evidence that tumors are angiogenesis dependent? J. Natl. Cancer Inst. *82*, 4–6.
32. van Iersel, M.L.P.S., Ploemen, J.H.T.M., Bello, M.L., Federici, G., and van Bladeren, P.J. (1997). Interaction of α, β-unsaturated aldehydes and ketones with human glutathione S-transferase P1–1. Chem. Biol. Interact. *108*, 67–78.
33. Luciani, N., Marie-Claire, C., Ruffet, E., Beaumont, A., Roques, B.P., and Fournie-Zaluski, M.C. (1998). Characterization of Glu^{350} as a critical residue involved in the N-terminal amine binding site of aminopeptidase N (EC 3.4.11.2): insights into its mechanism of action. Biochemistry *37*, 686–692.
34. Burley, S.K., David, P.R., Sweet, R.M., Taylor, A., and Lipscomb, W.N. (1992). Structure determination and refinement of bovine lens leucine aminopeptidase and its complex with bestatin. J. Mol. Biol. *224*, 113–140.
35. Logan-Smith, M.J., Lockyer, P.J., East, J.M., and Lee, A.G. (2001). Curcumin, a molecule that inhibits the Ca^{2+}-ATPase of sarcoplasmic reticulum but increases the rate of accumulation of Ca^{2+}. J. Biol. Chem. *276*, 46905–46911.
36. Kim, J.H., Shim, J.S., Lee, S.K., Kim, K.W., Rah, S.Y., Chung, H.C., and Kwon, H.J. (2002). Microarray-based analysis of anti-angiogenic activity of demethoxycurcumin on human umbilical vein endothelial cells: crucial involvement of the down-regulation of matrix metalloproteinase. Jpn. J. Cancer Res. *93*, 1378–1385.
37. Zhang, F., Altorki, N.K., Mestre, J.R., Subbaramaiah, K., and Dannenberg, A.J. (1999). Curcumin inhibits cyclooxygenase-2 transcription in bile acid- and phorbol ester-treated human gastrointestinal epithelial cells. Carcinogenesis *20*, 445–451.
38. Shim, J.S., Kim, D.H., Jung, H.J., Kim, J.H., Lim, D.Y., Lee, S.K., Kim, K.W., Ahn, J.W., Yoo, J.S., Rho, J.R., et al. (2002). Hydrazinocurcumin, a novel synthetic curcumin derivative, is a potent inhibitor of endothelial cell proliferation. Bioorg. Med. Chem. *10*, 2439–2444.
39. Kwon, H.J., Kim, M.S., Kim, M.J., Nakajima, H., and Kim, K.W. (2002). Histone deacetylase inhibitor FK228 inhibits tumor angiogenesis. Int. J. Cancer *97*, 290–296.
40. Jeong, J.W., Sohn, T.K., Yu, D.Y., and Kim, K.W. (2001). Membrane-type matrix metalloproteinase-1 induced invasive and angiogenic activities in chick chorioallantoic membrane (CAM) model. J. Korean Cancer Assoc. *33*, 49–55.